Journal Pre-proofs
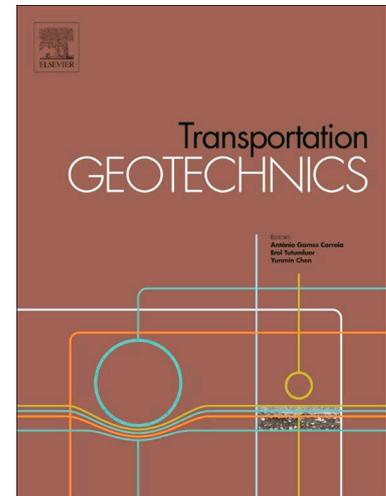
A new approach to particle shape classification of granular materials

Mohammad Ali Maroof, Ahmad Mahboubi, Ali Noorzad, Yaser Safi

Please cite this article as: M. Ali Maroof, A. Mahboubi, A. Noorzad, Y. Safi, A new approach to particle shape classification of granular materials, *Transportation Geotechnics* (2019), doi: https://doi.org/10.1016/j.trgeo.2019.100296

Article reference: TRGEO_2019_286

Article title: A new approach to particle shape classification of granular materials

Authors:

Mohammad Ali Maroof

Ph.D. Candidate, Faculty of Civil, Water and Environmental Eng., Shahid Beheshti University, Velenjak, Tehran, Iran, m_maroof@sbu.ac.ir

Ahmad Mahboubi (Corresponding Author)

Associate Prof., Faculty of Civil, Water and Environmental Eng.,
Shahid Beheshti University, Velenjak, Tehran, Iran
P.O. 16765-1719, E-Mail : a_mahboubi@sbu.ac.ir

Ali Noorzad

Associate Prof., Faculty of Civil, Water and Environmental Eng., Shahid Beheshti University, Velenjak, Tehran, Iran, a_noorzad@sbu.ac.ir

Yaser Safi

School of Dentistry, Shahid Beheshti University of Medical Sciences, Velenjak, Tehran, Iran, yaser_safi@yahoo.com

A new approach to particle shape classification of granular materials

M. Ali Maroof, Ahmad Mahboubi, Ali Noorzad, Yaser Safi

Abstract

The shape of soil particles influences asphalt, concrete, and soil behavior. The image analysis and visual comparison methods are commonly employed to quantify the shape characteristics of granular materials. However, previously introduced approaches have mostly been concerned with two-dimensional aspects and cannot specify the form and sphericity for entire grains. In this study, the shape of grains with various geometries is measured using a precise three-dimensional model for each particle extracted from X-ray computed tomography (micro-CT) images. A new sphericity ratio is proposed based on circumscribed and inscribed spheres. Further, a new sphericity class is developed which can be used for spherical to flat and ellipsoid to elongated particles. The results of various methods have been used and compared to quantify the sphericity. According to the results, the proposed approach outperforms other classifications. Furthermore, new charts have been suggested for quantitative-qualitative particle properties according to sphericity, roundness, and roughness, which can further be used for visual comparison.

Keywords: Particle shape, Sphericity, Roundness, Roughness, CT scan, Image processing, visual comparison.

1. Introduction

Particle shapes have a key role in determining the grain assemblies' behavior. Accurate characterization and analysis of aggregates morphology is important for a more detailed consideration of granular materials performance. The effect of particle morphology on soil behavior has been examined in terms of different aspects such as void ratio, mechanical behavior, stiffness and shear strength [1,2]. Furthermore, the effect of particle shape on mechanical characteristics of cement-based materials [3], asphalt mixture properties [4], mechanical behavior, degradation and rheology of railway ballast [5,6] have been evaluated.

The shape of particles can be described by three distinct features from large to small scales including form and sphericity (overall shape), roundness (sharpness of particle corners), and roughness (surface texture) [7,8]. In addition, the flatness and elongation of particles are used to describe soil grains [9–11]. Sphericity, roundness, and roughness are independent properties, i.e. when one of the parameter varies, other two parameters may remain

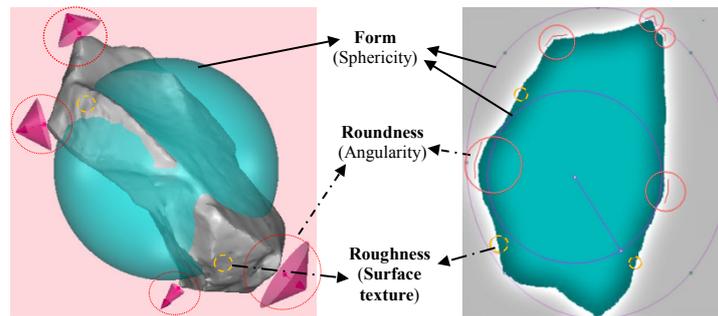unchanged [7]. These three features are illustrated in Figure 1.

Figure 1. Scale-dependent particle form, roundness, and roughness

Particle shape description could be done in two ways. In the two-dimensional (2D) expression, the particle shape is determined by the projection of the particle on a plane. The three-dimensional (3D) description is done using the CT scan images of particle or two orthogonal images [12]. Nevertheless, the use of 3D images is limited due to certain reasons such as sample dimensions, particle size, time, and cost despite the appropriate precision. Meanwhile, the 2D parameters presented to determine the particle shape are easily measurable by particle projection; however, their results are not reliable because of ignoring of the smaller size of particles (S) Indeed, the angle of projection may be chosen in a biased way and the projection outline cannot display the particle shape properly [13]; thus particle profiles may have a different shape and angularity across different orientations [14]. In practice particle morphology usually examined from particle projection images of the 3D particles. An approach to correlations between the 2D and 3D particle descriptors for irregular particles is proposed and validated [15]. This approach predicts the 3D size and shape descriptors from the cumulative distributions of the 2D descriptors that evaluated from the results of an all-around and random-projections [15].

Irregular particle shape is explained in three major forms of sphericity (versus oval or ellipse), roundness (versus angularity), and roughness (versus surface smoothness) in the following.

2. Particle shape characterization

2-1- Overall form

Overall form is often quantified by the sphericity, flatness, and elongation ratio. The degree of true sphericity is described as the ratio of the surface area of a sphere, of the same volume as the particle, to the particle surface area [16]. Obviously, the sphericity of disk-like bodies may seem the same as that of rod-like or bladed bodies in spite of their dissimilarities [17]. The uncertainty of definitions may seem confusing in terms of practical differences which are employed to describe particle forms [18]. Several researchers have tried to define the overall particle shape based on the longest, intermediate, and shortest orthogonal axes (L, I, S), which

might lead to the same results for different shapes [17]. Table 1 presents the different definitions for overall 2D and 3D shapes.

Table 1. Summary of relations for particle large scale description (form, sphericity)

Dimension	Particle shape description	Relation	Particle shape definition/description
3D	Elongation ratio, [19,20]	$\dfrac{S}{I}$	L: Longest axis, I: Intermediate axis, S: Short axis
	Flatness ratio, [19,20]	$\dfrac{I}{L}$	
	Flat and elongation ratio, [21]	$\dfrac{S}{L}$	
	Flatness index, [10]	$\dfrac{I+L}{2S}$	
	True sphericity, [22–24]	$\psi_s = \dfrac{S_s}{S_p} = \dfrac{\sqrt[3]{36\pi V_p^2}}{S_p}$	S_s : Surface of a sphere with same particle volume, S_p and V_p : Particle surface area and volume, respectively
	Sphericity, [23]	$\psi_v = \sqrt[3]{\dfrac{V_p}{V_c}}$	V_p : Particle volume , V_c : Volume of circumscribed sphere
	Intercept sphericity, [11]	$\sqrt[3]{\dfrac{IS}{L^2}}$	Equating the particle with an ellipsoid by large (L), medium (I) and small (S) diameter
	Corey shape factor, [25]	$\dfrac{S}{\sqrt{LI}}$	
	Maximum projection sphericity, [9]	$\sqrt[3]{\dfrac{S^2}{LI}}$	
	Working sphericity, [26]	$\dfrac{12.8\sqrt[3]{P^2 q}}{1 + p(1+q) + 6\sqrt{1 + p^2\left(1+q^2\right)}}$	p = S/I; q = I/L
	Scalene ellipsoid equivalent sphericity, [27]	$\dfrac{S}{L} = \dfrac{\left(W/nG_S\right)\left(6/\pi LI\right)}{L}$ $= \dfrac{6W}{nG_S IL^2}$	W: Sample weight, n: Number of particles, G_S : Specific gravity
2D	Form factor, [28]*	$\varphi_c = \dfrac{4\pi A}{P^2}$	P: Particle perimeter, A : Particle area
	Projection sphericity (circularity), [16,24]	$\psi_d = \dfrac{d_c}{D_c}$	d_c : Diameter of a sphere (circle in 2D) of the same volume (area) as the particle, D_c : Diameter of a circumscribed sphere (circle)
	Perimeter sphericity (Circularity), [16]	$C_r = \dfrac{P_c}{P_p}$	P_c : Perimeter of a circle of the same area as the particle, P_p : Particle perimeter
	Projection sphericity, [29]*	$\phi_s = \dfrac{A_p}{A_c}$	A_p : Particle area, A_c : Area of circumscribed circle
	Inscribed circle sphericity, [30]	$\varphi_0 = \sqrt{\dfrac{i}{D_c}}$	D_c : Diameters of circumscribed circle, i : Diameters of inscribed circle
	Circularity, [31]	$\dfrac{P_p^2}{A_p}$	P_p : Particle perimeter, A_p : Particle area

* Cox (1927) and Tickell (1931) have studied projection sphericity, however, called their measurement as "roundness" [30].

2-2-   Roundness

Roundness parameter is supposed to quantify whether the projections are sharp or round [23].

This feature was first distinguished from the concept of sphericity by Wadell (1933). He employed 2D projections of particles to define the roundness as the ratio of mean radius of corner curvatures to the maximum radius of inscribed circle [16]. Today, most researchers still use this definition of roundness [32] which refers to relative sharpness of particles on the corners and edges rather than their outline, resulting in the circularity in two dimensions or the sphericity in three dimensions [7]. The proposed relationships for describing and measuring roundness in 2D and 3D cases are presented in Table 2.

Table 2. Summary of relations for particle medium scale description (roundness)

Dimension	Particle shape description	Relation	Particle shape definition/description
3D	3D roundness, [33]	$R = \dfrac{\sum g(k)\left\|k_{max}\right\|^{-1}}{NR_{ins}}$	$g(k)$: Potential 'corner' at a given vertex on the surface, $\left\|k_{max}\right\|^{-1} = r_{min}$: Curvature radius, R_{ins} : Radius of the maximum inscribed sphere
	3D roundness, [13]	$R_{3D} = \dfrac{r^{3D_i}}{NR_{ins}}$	r^{3D_i} : The radius of the ith filling sphere obtained from the sphere-filling algorithm, N : Number of filling spheres, R_{ins} : Maximum inscribed sphere radius
2D	Roundness [10]	$\dfrac{r_1}{R} = \dfrac{2r_1}{D}$	r_1 : Radius of circle fitting sharpest corner, $D = 2R = \sqrt[3]{L \times I \times S}$: mean diameter of particle
	[23,24]	$P = \dfrac{\sum\left(\dfrac{r}{R}\right)}{N}, P = \dfrac{N}{\sum\left(\dfrac{r}{R}\right)}$	r: Radius of the corners, R : Radius of biggest inscribed circle, N: Number of corners (or small circle)
	Angularity, [17]	$A_{2D} = \dfrac{\sum\left[\left(180° - a°\right)x\right]}{r}$	a : bounding edge angle, x : Distance of the edges from the Centre of the maximum inscribed circle, r: Radius of the maximum inscribed circle
	Angularity Index, [34]	$AN = \dfrac{P_c}{P_e^2}$	P_c : Perimeter of the minimum convex boundary circumscribing an aggregate outline, P_e : Perimeter of an equivalent ellipse
	Angularity Index, [35]	$AI = \sum_{\theta=5}^{355} \dfrac{\left\|R_\theta - R_{EE\,\theta}\right\|}{R_{EE\,\theta}}$	R_θ : Radius of the particle at a directional angle θ , $R_{EE\,\theta}$: Radius of an equivalent ellipse (with same aspect ratio of the particle) at a directional angle θ
	Image J roundness	$\left(4A_P\right)/\left(\pi M^2\right)$	A_p : Particle area, M: Major axis

2-3- Surface roughness

The effect of surface roughness is addressed on a micro scale. Abrasion usually increases the surface roundness. On the other hand, weathering and crushing affect the surface texture both in terms of roundness and roughness by exposing a larger surface area and creating new corners [7].

The surface texture can be investigated through image processing techniques such as erosion and dilatation [36,37]. In erosion technique, a morphological process is employed to remove the boundary pixels of the target image and reduce the density of perimeter boundary. In dilatation technique, a reverse process is utilized to add pixels along the boundary [38].

Morphological image processing is used to quantify the morphology and texture of particles by Fourier transform, describing particle profile via an angle associated chord, and fractal dimension method [39,40]. Hyslip and Vallejo offered the area-perimeter method to evaluate the grain roughness from the fractal dimension (D_R) [41]. They found that coarser sands present larger D_R values [42].

Note that the current texture measurement methods employ a black and white, high-resolution image to assess the irregularity of particle boundary. Nevertheless, the impact of color variation and surface micro texture are not properly detected by popular techniques for image texture analysis [43].

A 3D fractal dimension is also proposed which can be used for fractal nature characterization of the surface textures associated with the actual sand particle morphology [33].

2D and 3D roughness is measured by comparing the real surface and real outline with the benchmark closed outline and benchmark closed surface, respectively. Benchmark closed outline reconstructed based on the Fourier analyses and benchmark surface reconstructed by the spherical harmonic analyses [44]. The total degree of spherical harmonic series and total number of harmonics, N, of 25 to minimize the influence of surface texture [40,44]. The proposed surface texture relationships are presented in Table 3 for 2D and 3D cases.

Table 3. Summary of proposed relations for particle roughness

Dimension	Particle shape description	Relation	definition
3D	Surface texture index, [45]	$STI_{3D} = \dfrac{V_1 - V2}{V_1} \times 100$	V_1: Volume of the 3D images, in voxel; and V_2: Volume of the 3D images after an opening operation, in voxel
2D	Roughness fractal dimension, [41]	$D_R = \dfrac{2}{m}$	m: Slope coefficient of logarithm relationship between particle area (A_p) and perimeter (P_p)
	Roughness, [46]	$R_0 = \dfrac{P}{\pi * D_{ave}}$	P: Particle perimeter, D_{ave}: Average diameter of the two orthogonal planes
	Roughness, [31]	$\dfrac{P_p}{P_{conv.}}$	P_p: Particle perimeter, $P_{conv.}$: Convex hull perimeter
	Surface parameter, [36]	$SP = \dfrac{A_1 - A_2}{A_1} \times 100$	A_1 and A_2: Areas of objects on an image before and after the erosion-dilation cycles, respectively
2D	Sphericity (first and second harmonics)	$R(\theta) = a_0 +$	$R(\theta)$: The radius at angle θ, N: total number of harmonics, n: Harmonic number, a and b: factors giving the magnitude and phase for each harmonic
	Roundness (higher harmonics, around 16th) [47]	$\displaystyle\sum_{i=1}^{N}(a_n \cos n\theta + b_n \sin n\theta)$	
	Surface texture (much higher harmonics)		

The methods for shape description include particle shape quantification by direct measurement, visual comparison and measurement in response to a set of standard physical conditions such as settling velocity in water [48]. The relationships for particle shape quantification, presented in the previous section, visual description and image processing are explained further.

2-4- Characterization method

2-4-1- Visual description

In large number of particles (field measurements and soil samples) and particles with a large size (gravels and boulders), the quantitative description of particles shape is too difficult; therefore, some researchers have suggested charts for visual comparison, and description of the particle shape. These charts could facilitate the estimation of particle roundness and sphericity using visual comparisons, which presenting reference particle silhouettes [18]. Zingg [19] classified the particles using the elongation ratio ($\frac{I}{L}$) and flatness ratio ($\frac{S}{L}$). Krumbein [11] presented a comparison chart for roundness. Powers [49] proposed a roundness scale for visual comparisons and manual determination values of roundness and sphericity (Figure 2). Also, Krumbein and Sloss [50] suggested the combination of sphericity and circularity of particles to estimate the shape of particles. Then, Cho et al. [51] modified this chart by defining the regular parameter of the shape of particle as the circular and spherical arithmetic mean, $\xi = \frac{\rho + s}{2}$, and adding the diagonal dotted line to the proposed shape. Lees [17] suggested a chart for visual 2D estimation of angularity of particles. Blott and Pye [21] developed the studies of Zingg [19] as well as Sneed and Folk [9] and presented some graphs for describing the shape of particles.
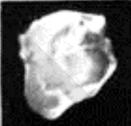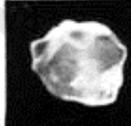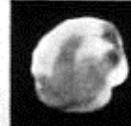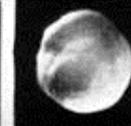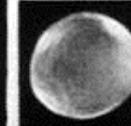
Roundness class	Very Angular	Angular	Sub Angular	Sub Rounded	Rounded	Well Rounded
High sphericity						
low sphericity						
Roundness indices	0.12-0.17	0.17-0.25	0.25-0.35	0.35-0.49	0.49-0.70	0.70-1.0
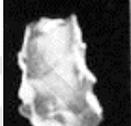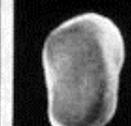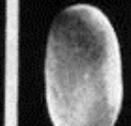
Figure 2. Power's roundness class [49]

Today the primary definitions and subjective chart methods are broadly used to classify sphericity and roundness of particles by visual comparisons [18]. In a sample, the number of particles belonging to the same class is multiplied by the geometric mean of each class. Next, the sum of products is divided by the total number of particles in order to calculate the mean sphericity and roundness [49]. Based on the proposed approaches and graphs, the same visual description is implemented in the present study.

2-4-2- Imaging and image processing

Image processing and image analysis methods have been developed in recent decades to quantify the particle shape. There are more limitations for the particles with a large size

(gravels) and field measurements. In addition, many image processing methods specify the 2D particle shape [21]. The particle shape can be measured using two dimensional, three dimensional and orthogonal images. In 2D approaches, the geometric characteristics of particles are obtained through processing digital images taken by camera for large particles and by microscope for particles smaller than millimeters. The scanning electron microscopy (SEM) and transmission electron microscopy (TEM) are two common microscopic imaging techniques [52].

On the other hand, 2D imaging cannot illustrate the specification of particle forms as they are often placed on larger dimensions and the smaller size might be ignored; particle projection may also be changed by particle rotation or image capture direction. Thus, to resolve the two-dimensional limitations, 3D particle morphology is performed using a three-dimensional X-ray computed micro-tomography (μCT). Micro CT scan is a non-destructive method which can determine the 3D structure of particle samples using computed tomography. 3D images can be obtained by three types of micro-CT scan including medical CT device, industrial X-ray generation tube, and synchrotron micro tomography [53].

Methods to reconstruction and quantify of 3D particle surfaces from its μCT images can be classified into three groups: direct calculating from voxel assemblies of images, reconstructed surface with composed of triangular surface meshes, and quantifying from the particles surface reconstructed from 3D spherical harmonic functions [54,55].

The volume and surface area can be measured using the total number of voxels (3D pixels) and voxels of boundaries, respectively, through analyzing of micro CT scan images [33]. Furthermore, the 3D image of particles is determined by two orthogonal images or two images from two different angles. Zheng and Hryciw [56] determined the shape and size of particles by taking two parallel images through stereophotography.

Engineering classification of grains is generally based on particle size distribution and relative density, without considering the real particle morphology which gives emphasizes the requirement of a standard procedure for sphericity, roundness, and roughness quantification. In addition, insufficient models and relationships might arise from the complexity and variety of grain shapes and characterizing proper shape descriptors for modeling. On the other hand, despite the appropriate precision in three-dimensional imaging, the applicability is restricted due to reasons such as sample dimensions, particle size, time, and cost.

In this study, different shapes of gravel are evaluated. Particle geometries are measured using ImageJ software in 2D [57] and three dimensional imaging via X-ray computed micro-tomography (μCT). In practice, visual comparison methods are adopted in the form of visual charts. In this way, quantitative-qualitative particle sphericity, roundness, and roughness classifications are proposed. The proposed diagrams can be used for rough estimations along with the image processing technique, as a more precise method, to describe and quantify the

shape of material particles.

3. Materials and Methodology

The shape of gravel particles, 15 mm mean diameter ($\frac{1}{2}$ to $\frac{3}{4}$ inches), is investigated. Solids may have different shapes; in order to evaluate their form, it is necessary to adopt a standard shape for comparison. In this regard, sphere may properly be taken as a standard shape for comparison [49]. Also, sedimentary particles sometimes have an ellipsoid shape; therefore, in this study, particle shapes are categorized in two groups: spherical and ellipsoid; (Figure 3 and Figure 4).

The first particle assessed in this study is a glass bead, referred to as particle No. 1 in Figure 3. Furthermore, rounded spherical and ellipsoid grains were provided from sedimentary quartz particles. In addition, angular spherical and ellipsoid grains were collected from crushed aggregate. Flat and flat-elongated particles were taken from metamorphic rocks (slate).

In this research, a new classification is developed based on 3D combination of classification methods of Powers [49] and Krumbein and Sloss [50]. Particles are classified according to their sphericity and roundness in six groups for spherical particles and four groups for ellipsoid particles; particles 1 to 36 are spherical (equant) while particles 37 to 60 are ellipsoid. Particles are placed in classes based on visual comparison, Powers class, and sphericity class as presented in Figure 3.

The grains are grouped such that they present the particle form, roundness, and surface roughness characteristics. For spherical and ellipsoid particles in each group, the sphericity decreases from left to right where the left and right grains are the most spherical and flat grains, respectively. Further, the particle angularity and roughness increase in a descending order, such that the uppermost particle is rounded and smooth while the lowest grain is angular and rough .

Particle shapes are analyzed in 2D and 3D. Two-dimensional particle shapes are measured by the ImageJ software; an open source image processing software [57]. Particle shape analysis requires binary images, black and white, and distinguishing the particle boundary by thresholding [57]. This software can measure particle shape as the following items [57]: particle number, area, perimeter, major and minor axis lengths of the fit ellipses, circularity; similar to Cox's definition [28], aspect ratio (AR; major axis length of approximate ellipse divided by minor axis length of approximate ellipse) and roundness ($4[Area]/\pi[Major\,axis]^2$). Figure 3 displayed the particle projection scaled by ImageJ software.
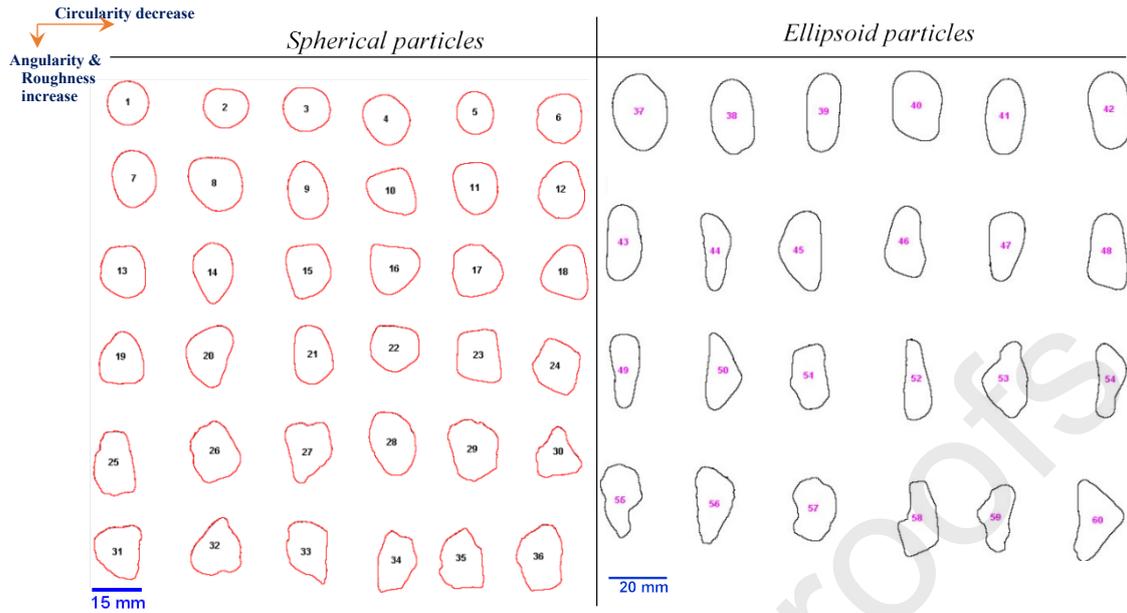
Figure 3. Particles projection used for analysis in two dimensional, Particles circularity, roundness and roughness variation shown in top and particle number is shown within particle outline

On the other hand, 3D particle morphology is developed from X-ray computed tomography (CT) images. the image processing is then performed to retrieve the particle surface information using OnDemand3D application [58]. Particle dimensions, as well as particle surface area and volume are measured using this software. As an important step in the geometric modeling, a polygonal mesh of iso-surface is derived from the 3D scalar voxels for surface reconstruction. Hence, one or a number of phases can be isolated or rendered within the data set [59]. Note that 3D particle surface is reconstructed by 3DimViewer software [60] with the results demonstrated in Figure 4.
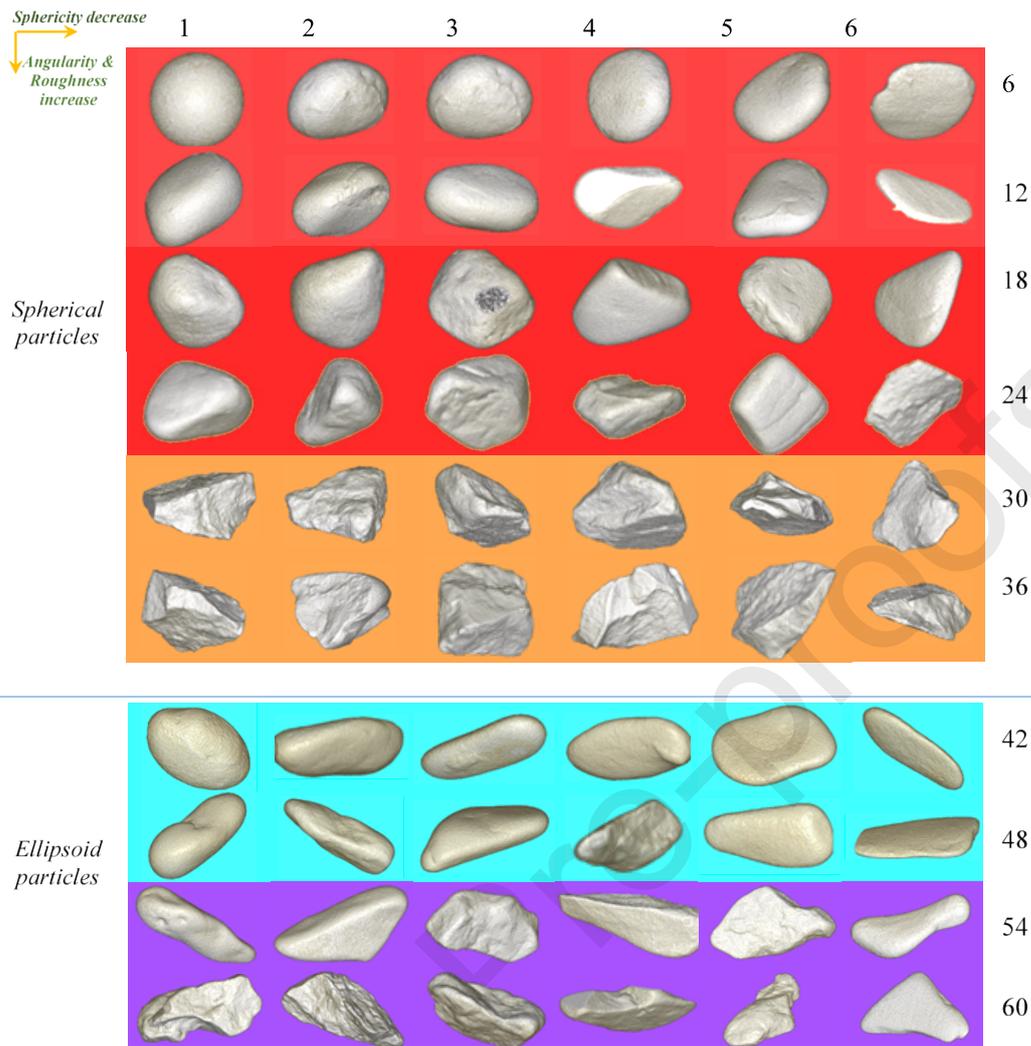
Figure 4. 3D representation of spherical and ellipsoid particles used for analysis. Particles sphericity, roundness and roughness variation shown in top and particles numbers are given in top and right

For all particles, particle dimensions including L, I, and S are measured in three orthogonal axes. Subsequently, Wadell's roundness, circumscribed and inscribed circle's diameter, circumscribed and inscribed sphere's diameter, and the diameter of sphere with the same area and volume as particle are measured. These parameters as well as maximum particle projection, outline and 3D view of particle are illustrated for particle No. 34 in Figure 5.
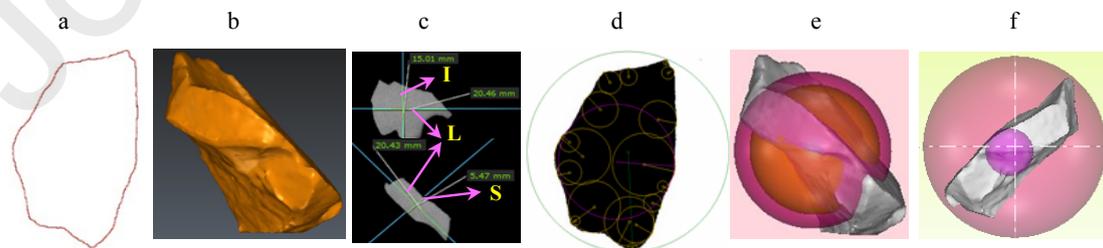
Figure 5. Particle No. 34, a: maximum particle projection, outline, b: 3D view, c: particle dimensions, L, I, S, d: particle projection, Wadell's roundness, circumscribed and inscribed circles, e: Sphere with same area (inner sphere) and same volume as particle (outer sphere), f: largest inscribed and smallest circumscribed sphere, this study

4. Results and discussion

Particle shape is described in three major forms: sphericity, roundness and roughness. In this section, these three features are calculated and described. The new class for sphericity proffer and then new charts will be presented for describing sphericity, roundness, and roughness.

4-1- Particles' form and sphericity

Overall particle shape is measured in terms of two categories; sphericity and form. Various sphericity and form factors of 10 particle groups have been investigated, each of which contains 6 particles.

In this section, a new sphericity is proposed and the results were compared with other sphericity and form relationships in the literature.

4-1-1- Sphericity

In this study, a new method is suggested to determine the sphericity of particles, referred to as inscribed-circumscribed sphere ratio, $\psi_{i-c} = \dfrac{d_{i-s}}{d_{c-s}}$; where d_{i-s} and d_{c-s} are the diameters of largest inscribed sphere and smallest circumscribed sphere, respectively.

For regular particle shapes, such as sphere, ellipsoid and oblate, the inscribed sphere diameter is approximately equal to the smallest dimension, S, while for irregular shapes, it is often larger than the smallest grain axis. The diameter of minimum circumscribed circle and the largest dimension of the grains are mostly similar (Figure 6); however, the d_{c-s} is predominantly greater than these parameters. The inscribed circle can be achieved in 2D particle outline, which is not associated with the actual grain shape; and therefore, it cannot be a proper parameter for particle shape assessment as with inscribed circle sphericity suggested by Riley [30].
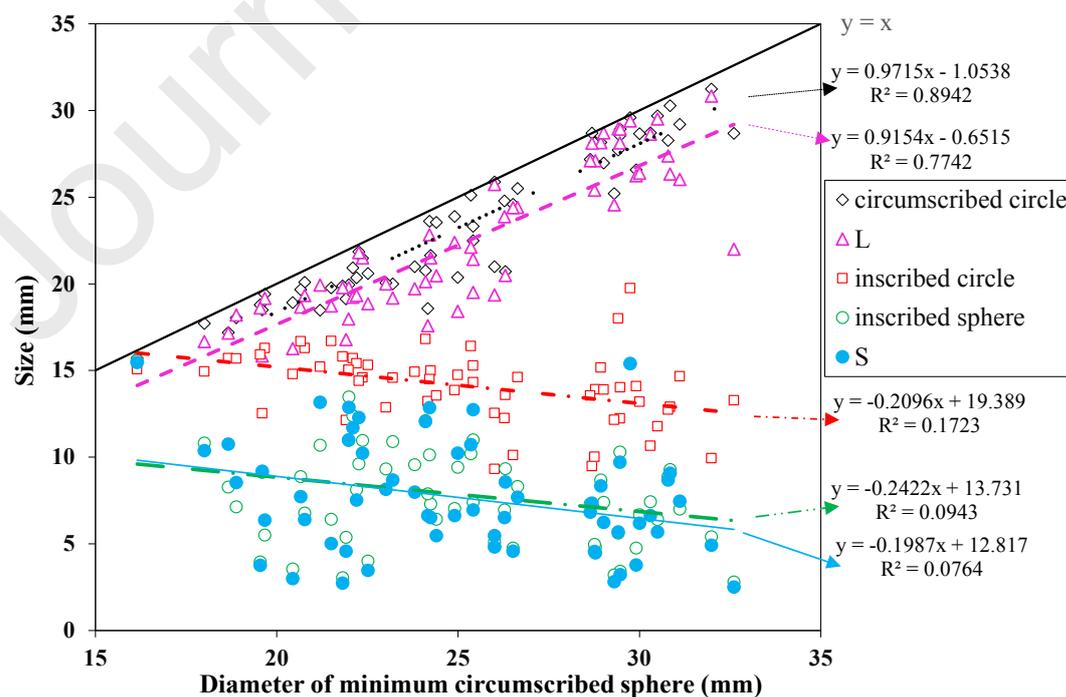
Figure 6. Inscribed and circumscribed circles diameter, inscribed spheres diameter, small and long dimension of particles versus circumscribed spheres diameter

Particle sphericity based on Wadell projection sphericity (ψ_d), Wadell true sphericity (ψ_s), Riley inscribed circle sphericity (φ_0), and inscribed-circumscribed sphere ratio (ψ_{i-c}) have been measured and presented in Figure 7. φ_0 measured in 2D indicates similar sphericity for particles with an identical outline. Note that 2D parameters are generally different from natural grain shapes. Although ψ_s, ψ_d and ψ_{i-c} have a similar trend, they produce the highest to lowest values, respectively. ψ_{i-c} decreases as elongation increases and for spherical and ellipsoid particles, ψ_{i-c} presents a good agreement with spherical and flat particle. This ratio can also be appropriately employed for ellipsoid and elongated particles.
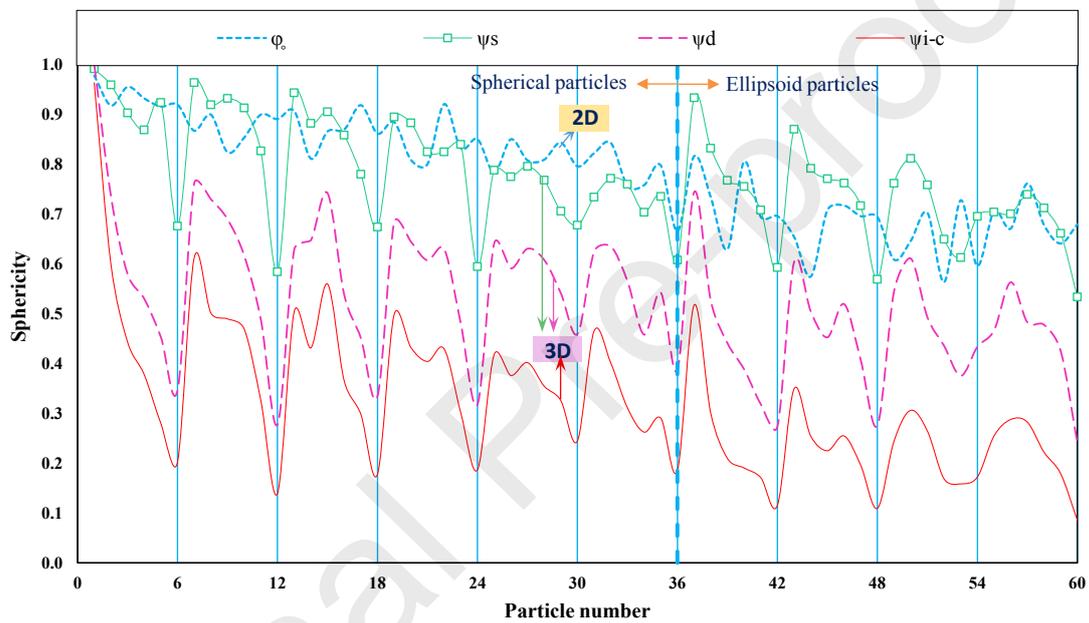
Figure 7. Inscribed sphere sphericity (ψ_{i-c}) with Wadell projection sphericity (ψ_d), Wadell true sphericity (ψ_s), Riley inscribed circle sphericity (φ_0)

4-1-2- Form

For overall grain shape measurement, the form factor is also provided. Blott and Pye (2007) modified Sneed and Folk and Zingg diagrams and classified particle forms based on the following: elongation ratio (I/L) and the flatness ratio (S/I) as the equant spheroid, flat spheroid, discoid, prolate spheroid, blade, and roller for rounded particles, while the equant block, flat block, very oblate spheroid, plate, elongate block, blade and rod for non-rounded particles [21]. Based on this method, overall form of 6 particle groups is shown in Figure 8. This classification represents only the overall form (sphericity) and does not provide any further information on smaller scales (roundness and roughness).
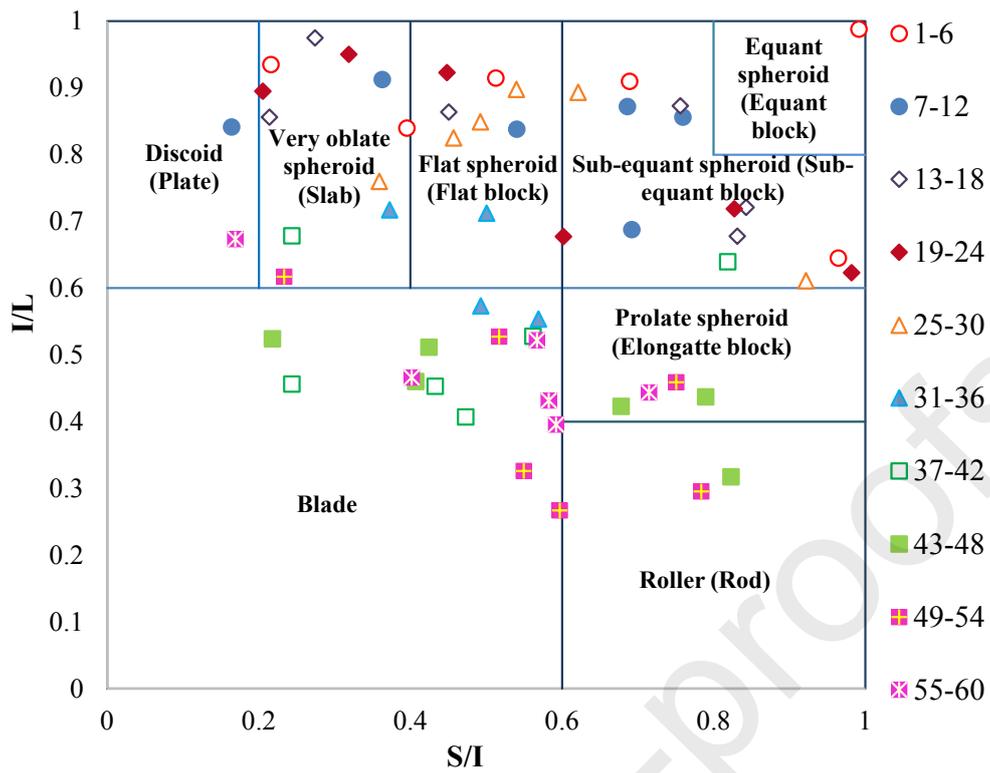
Figure 8. Blott and Pye particles form description for rounded and non-rounded particles

Form factors considered here and compared include: elongation ratio, flatness ratio, elongation and flatness ratio, Sneed and Folk maximum projection sphericity, Aschenbrenner working sphericity, Krumbein intercept sphericity and Corey shape factor (Figure 9 and Figure 10). All these form factors have a similar trend, except for elongation ratio and flatness ratio. The results indicate that Aschenbrenner, Krumbein, Sneed and Folk and Corey shape factors, Wentworth flatness index, elongation and flatness ratio, and ψ_{i-c} offer the highest values of sphericity, respectively. As can be seen in Figure 9 and Figure 10, the elongation and flatness ratios (S/L) is similar to ψ_{i-c}, especially for ellipsoid particles.

ψ_{i-c} can be a good representative of the actual grain shape, from spherical to flat, and ellipsoid to elongated particles. A new sphericity class will be investigated quantitatively in the following sections. It was observed that the proposed sphericity ratio with sphericity class outperforms other sphericity and form factors.
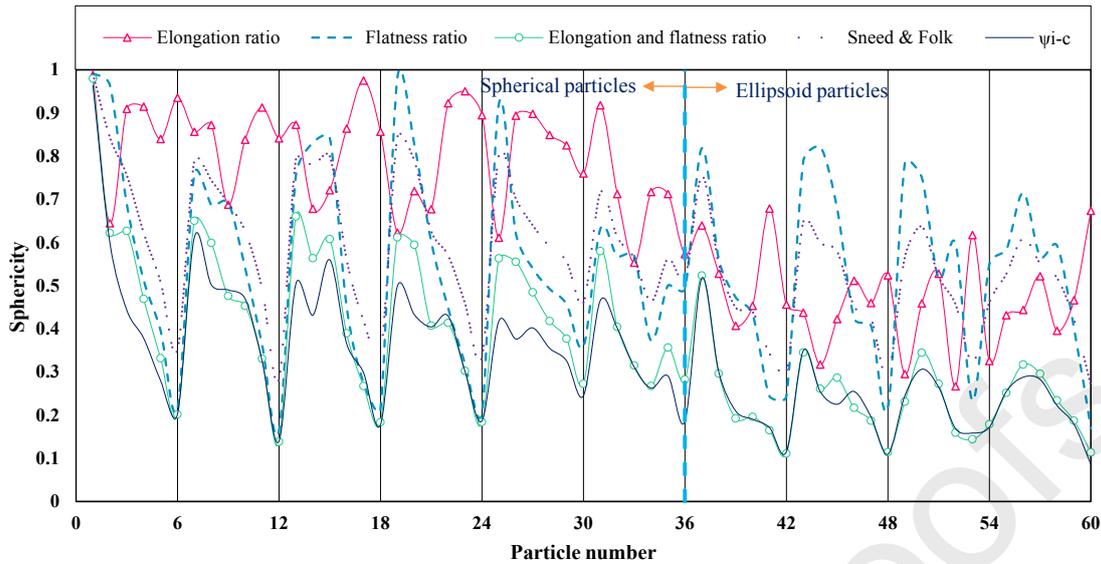
Figure 9. Inscribed-circumscribed sphere ratio (ψ_{i-c}) with particles elongation, flatness, elongation and flatness ratio, Sneed and Folk maximum projection sphericity
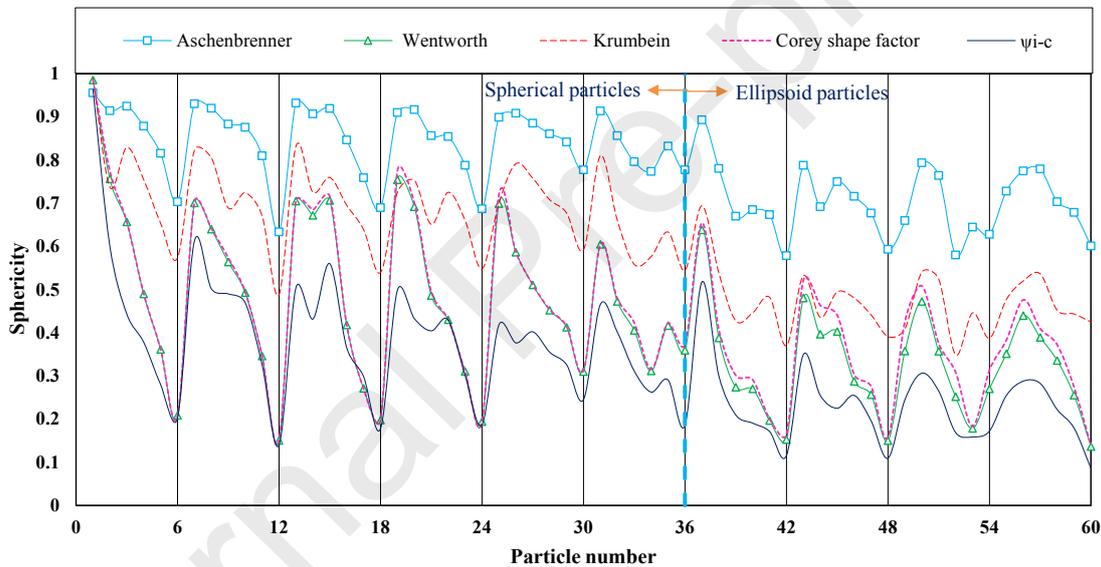
Figure 10. Inscribed-circumscribed sphere ratio (ψ_{i-c}) with, Aschenbrenner working sphericity, Wentworth flatness index, Krumbein intercept sphericity and Corey shape factor

4-2- Particles roundness

Particle roundness is calculated using Wadell's roundness, ImageJ software roundness and Cox circularity through image analysis, as depicted in Figure 11. For spherical rounded particles, the results represent that the methods of Cox, Wadell and ImageJ roundness produce similar results; as the particle roundness decreases, more dissimilar results are obtained. For ellipsoid particles, these methods have different values.

Wadell claimed that the roundness of particles could be measured unbiasedly through 2D projection [23]. To calculate the roundness using this method, the algorithms proposed by Zheng and Hryciw (Zheng and Hryciw 2015) as well as Nie et al. [61] can be used. Despite the difficulty of calculating the particle roundness by Wadell method and 2D framework,

Wadell method proffer a good agreement with the roundness of different particle groups. The 3D reference surfaces (e.g. spheres of various radii) should be fitted to the corners of pebble surface for accurate assessment of 3D roundness [7]; A similar method is suggested by Nie et al. [13].
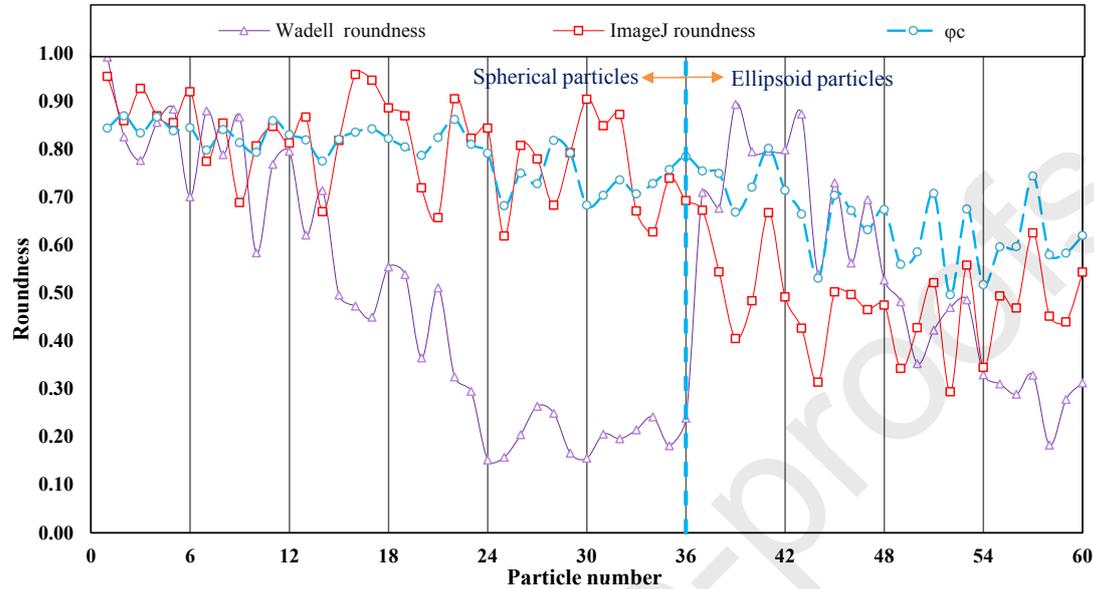
Figure 11. Particles Wadell roundness, ImageJ software roundness, and Cox formula (φ_c)

4-3- Particles roughness (surface texture)

It is hard to measure the roughness due to its scale dependency [2] and almost all of the existing methods for soil grains roughness description are qualitative. Porter classified the sand particle surface texture under five textural groups: abraded, lobate, corroded, smooth and faceted [62]. Barksdale and Itani used a roughness scale to examine the surface texture of aggregates visually from glassy to very rough [63]. ASTM D5821 categorized the coarse aggregate under smooth and rough surfaces [64]. BS 812 classified the surface texture as glassy, smooth, granular, rough, crystalline and honeycombed [65].

In order to provide a graph for the visual estimation of grain shape for practice, a visual method with respect to qualitative classification was proposed. Because of the shortcomings of surface texture quantitative relationships, particle roughness descriptive terms have been chosen based on qualitative suggestions; this classification was adopted using Porter method and BS 812 standard. The surface roughness is classified under six groups: very rough, rough, relatively rough, corroded, smooth, and glassy.

4-4- Particle shape classification

Numerous studies have been done on measuring the soil grains morphology. However, given the lack of a standard for the quantity and quality of grain and the difficulty of measuring the shape of the grains in practice, it is required to redefine particle shape classifications.

Particle forms are measured by inscribed-circumscribed sphere ratio and classified based on visual adaptation in seven classes for spherical (equant) particles: discoid (plat), slab, flat, low sphericity, medium sphericity, spherical (equant) and high sphericity along with five classes for ellipsoid (elongated) particles: flaky-elongated (blade), elongated (rod), moderately elongate, prolate and elliptical.

Particle roundness is measured by Wadell roundness and classified as Powers verbal class [49]. This roundness scaling is graded into very angular, angular, sub-angular, sub-rounded, rounded and well rounded.

Particle sphericity, roundness, and roughness are classified quantitatively and qualitatively, as presented in Table 4. Each particle is assigned to one of the classes, depending on the particle image which most closely resembles it.

Table 4. Particles sphericity, roundness and roughness quantitative-qualitative classification

Sphericity class	0-0.07	0.07-0.15	0.15-0.25	0.25-0.35	0.35-0.45	0.45-0.60	0.60-0.80	0.80-1.0
Form (spherical particle)	Unnatural particle	Discoid (plat)	Slab	Flat	Low sphericity	Medium sphericity	Spherical (equant)	High sphericity
Particle image								
Form (ellipsoid particle)	Unnatural Particle	Flaky-elongated (blade)	Elongated (rod)	Moderately elongate	Prolate	Elliptical	-	-
Particle image							-	-

Roundness	Unnatural particle	Very angular	Angular	Sub angular	Sub rounded	Rounded	Well rounded
Roundness class	0.0-0.12	0.12-0.17	0.17-0.25	0.25-0.35	0.35-0.49	0.49-0.70	0.70-1.0
Particle image							

Roughness		Very rough	Rough	Relatively rough	Corroded	Smooth	Glassy
Particle image							
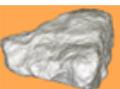
Table 5 presents the particle dimensions, area, perimeter, surface area and volume,

circumscribed and inscribed circles, circumscribed and inscribed spheres and Wadell roundness. Also, the particle sphericity, roundness and roughness are classified in the same table.

Particle number	Measured value													Particle shape description		
	S (mm)	I (mm)	L (mm)	Ap (mm2)	Pp (mm)	Vp (mm3)	Sp (mm2)	Wadell Roundness	Dins-cir (mm)	Dcir-cir (mm)	Dins-sph (mm)	Dcir-sph (mm)	ψi-c	Sphericity	Roundness	Roughness
1	15.5	15.6	15.8	194.7	51.2	1970.1	766.1	0.99	15.1	15.7	15.6	16.2	0.96	High sphericity	Well rounded	Glassy
2	10.4	10.8	16.7	193.7	50.3	1652.0	704.1	0.83	14.9	17.7	10.8	18.0	0.60	Spherical (equant)	Well rounded	Relatively smooth
3	10.8	15.6	17.2	225.8	55.4	1522.4	708.2	0.78	15.7	17.2	8.3	18.7	0.44	Low sphericity	Well rounded	Relatively smooth
4	8.5	16.7	18.2	171.1	47.3	1275.8	654.1	0.86	16.3	19.4	7.1	18.9	0.38	Low sphericity	Well rounded	Smooth
5	6.4	16.1	19.2	243.4	57.4	939.9	502.0	0.88	15.7	18.0	5.5	19.7	0.28	Flat	Well rounded	Smooth
6	3.8	17.4	18.6	243.3	57.1	774.9	603.1	0.70	15.9	18.8	4.0	19.5	0.20	Slab	Well rounded	Smooth
7	12.9	16.9	19.8	266.5	61.5	2884.6	1016.0	0.88	15.0	20.0	13.5	22.0	0.61	Spherical (equant)	Well rounded	Smooth
8	12.1	17.6	20.1	317.3	65.4	2380.9	937.1	0.79	16.8	20.8	12.1	24.1	0.50	Medium sphericity	Well rounded	Relatively smooth
9	10.2	14.8	21.5	248.6	58.9	2097.7	849.7	0.87	14.6	21.5	11.0	22.4	0.49	Medium sphericity	Well rounded	Smooth
10	8.7	16.1	19.2	237.5	58.2	2887.5	1073.1	0.58	14.6	20.0	10.9	23.2	0.47	Medium sphericity	Well rounded	Smooth
11	6.4	17.6	19.3	254.4	57.9	1394.9	729.9	0.77	16.3	20.1	6.8	20.8	0.33	Flat	Well rounded	Relatively smooth
12	2.7	16.7	19.8	271.6	60.9	690.1	646.2	0.80	15.8	19.9	3.1	21.8	0.14	Discoid (plat)	Well rounded	Smooth
13	13.2	17.4	19.9	260.8	60.1	2567.0	960.5	0.62	15.2	18.5	10.7	21.2	0.50	Medium sphericity	Rounded	Corroded
14	12.3	14.8	21.8	241.1	59.4	1706.3	782.3	0.71	14.4	21.9	9.6	22.3	0.43	Low sphericity	Well rounded	Corroded
15	11.7	13.9	19.2	260.3	60.0	2425.1	963.7	0.50	15.7	20.9	12.4	22.1	0.56	Medium sphericity	Rounded	Relatively rough
16	7.5	16.7	19.3	262.3	59.7	1793.2	830.6	0.47	15.4	20.4	8.1	22.2	0.37	Low sphericity	Sub rounded	Relatively smooth
17	5.0	18.3	18.7	282.9	61.7	1504.0	813.3	0.45	16.7	19.8	6.4	21.5	0.30	Flat	Sub rounded	Corroded
18	3.5	16.2	18.9	258.8	59.7	895.6	666.3	0.56	15.3	20.6	4.0	22.5	0.18	Slab	Rounded	Relatively smooth
19	11.0	11.2	18.0	250.3	59.4	2151.1	900.0	0.54	15.0	19.2	11.0	22.0	0.50	Medium sphericity	Rounded	Relatively smooth
20	12.7	15.4	21.4	281.2	63.7	2592.4	1032.6	0.37	15.3	23.3	11.0	25.4	0.43	Low sphericity	Sub rounded	Relatively rough
21	8.2	13.5	20.0	249.4	58.6	1883.2	893.4	0.51	12.9	20.1	9.3	23.0	0.40	Low sphericity	Rounded	Relatively rough
22	7.7	17.2	18.7	247.3	57.1	1463.4	755.3	0.33	16.7	19.7	8.9	20.7	0.43	Low sphericity	Sub angular	Relatively rough
23	6.5	20.4	21.5	274.1	62.0	1839.7	863.8	0.30	15.0	21.6	7.3	24.2	0.30	Flat	Sub angular	Corroded
24	3.0	14.6	16.3	256.4	60.6	718.1	651.8	0.15	14.8	20.4	3.5	18.9	0.19	Slab	Very angular	Rough
25	12.9	14.0	22.8	286.7	69.0	2060.8	992.8	0.16	14.5	23.6	10.1	24.2	0.42	Low sphericity	Very angular	Very rough
26	10.2	16.5	18.4	297.4	67.1	2106.4	1024.4	0.21	14.7	20.4	9.4	25.0	0.38	Low sphericity	Angular	Very rough
27	10.7	19.9	22.1	278.1	65.8	2210.3	1030.4	0.26	16.4	25.1	10.2	25.4	0.40	Low sphericity	Sub angular	Rough
28	8.6	17.4	20.5	307.5	65.3	1892.5	962.8	0.25	13.6	20.7	9.3	26.3	0.36	Low sphericity	Angular	Very rough
29	6.6	14.5	17.6	320.4	67.7	1610.5	940.5	0.17	13.2	18.6	7.9	24.2	0.33	Flat	Very angular	Rough
30	4.6	12.8	16.8	201.1	57.8	832.9	631.4	0.16	12.1	19.1	5.4	21.9	0.25	Slab	Very angular	Rough
31	9.2	14.5	15.8	274.7	66.5	1628.4	911.2	0.21	12.5	18.5	9.1	19.6	0.47	Medium sphericity	Angular	Rough
32	8.0	14.1	19.7	267.9	64.3	1779.7	919.8	0.20	14.9	21.0	9.6	23.8	0.40	Low sphericity	Angular	Very rough
33	7.7	13.5	24.4	261.8	64.8	1652.1	888.6	0.22	14.6	25.5	8.3	26.6	0.31	Flat	Angular	Rough
34	5.5	14.7	20.5	237.7	60.9	1429.2	871.2	0.24	13.6	23.5	6.4	24.4	0.26	Flat	Angular	Rough
35	7.0	13.9	19.5	277.4	64.4	1318.7	790.3	0.18	14.3	22.5	7.4	25.4	0.29	Flat	Angular	Very rough
36	5.5	11.1	19.4	320.0	68.0	1012.4	801.5	0.24	9.3	21.0	4.8	26.0	0.19	Slab	Angular	Rough
37	15.4	18.8	29.4	404.2	77.9	4631.1	1438.6	0.71	19.7	29.6	15.4	29.7	0.52	Medium sphericity	Well rounded	Relatively smooth
38	8.3	14.9	28.1	324.6	70.1	2350.3	1026.5	0.68	15.2	28.2	8.7	28.9	0.30	Flat	Rounded	Smooth
39	5.7	12.0	29.5	284.9	69.5	1595.0	859.1	0.89	11.8	29.7	6.4	30.5	0.21	Slab	Well rounded	Relatively smooth
40	5.7	13.1	29.0	301.2	68.8	1571.6	864.8	0.80	18.0	27.7	5.6	29.4	0.19	Slab	Well rounded	Relatively smooth
41	4.5	18.4	27.1	364.4	71.8	1783.6	1003.9	0.80	13.9	28.8	4.8	28.0	0.17	Slab	Well rounded	Smooth
42	3.2	13.2	28.9	323.0	71.6	1008.3	819.6	0.80	14.0	28.9	3.4	29.5	0.12	Discoid (plat)	Well rounded	Smooth
43	9.7	12.3	28.1	273.7	68.3	2589.8	1047.2	0.87	12.2	28.6	10.3	29.5	0.35	Flat	Well rounded	Smooth
44	7.5	11.0	26.0	319.8	71.8	1936.6	974.2	0.54	14.7	29.2	7.0	31.1	0.23	Slab	Rounded	Smooth
45	7.3	8.9	28.1	198.5	65.1	1584.0	829.6	0.73	9.5	28.7	7.3	28.7	0.25	Flat	Well rounded	Corroded
46	6.2	14.7	28.7	266.1	67.0	1507.9	833.5	0.56	13.9	27.0	7.4	29.0	0.26	Flat	Rounded	Relatively rough
47	4.8	11.8	25.7	240.9	65.7	1026.9	686.4	0.69	12.5	25.9	5.1	26.0	0.20	Slab	Rounded	Smooth
48	2.8	12.9	24.6	303.8	71.5	820.1	744.1	0.53	12.2	25.2	3.2	29.3	0.11	Discoid (plat)	Well rounded	Relatively smooth
49	6.6	8.5	28.6	208.0	64.9	1313.8	761.2	0.48	10.7	28.7	7.4	30.3	0.24	Slab	Sub rounded	Corroded
50	9.1	12.1	26.3	228.1	66.5	1828.7	890.1	0.35	12.9	30.8	9.3	30.3	0.31	Flat	Sub rounded	Relatively rough
51	6.5	12.6	23.9	242.6	62.3	1468.1	822.9	0.42	12.3	24.8	7.0	26.3	0.26	Flat	Sub rounded	Relatively rough
52	4.9	8.2	30.8	207.1	68.8	993.7	740.9	0.47	9.9	31.2	5.4	32.0	0.17	Slab	Sub rounded	Corroded
53	3.8	16.2	26.2	284.5	69.1	1056.2	817.7	0.49	14.1	26.6	4.8	29.9	0.16	Slab	Sub rounded	Relatively rough
54	4.6	8.3	25.4	195.3	65.4	781.2	589.4	0.33	10.0	28.1	5.0	28.8	0.17	Slab	Sub angular	Relatively smooth
55	6.8	11.7	27.1	247.8	68.6	1998.8	1088.8	0.31	13.5	27.2	7.3	28.6	0.25	Flat	Sub angular	Very rough
56	8.7	12.2	27.4	264.3	70.9	2039.6	1109.7	0.29	12.7	28.3	8.9	30.8	0.29	Flat	Sub angular	Very rough
57	6.6	11.7	22.4	265.1	63.6	1618.0	900.5	0.33	13.9	23.9	7.0	24.9	0.28	Flat	Sub angular	Rough
58	6.2	10.4	26.4	254.5	70.5	1419.4	856.8	0.18	13.2	28.7	6.7	30.0	0.22	Slab	Angular	Corroded
59	4.6	11.4	24.4	199.3	62.2	726.8	590.8	0.28	10.1	24.6	4.8	26.5	0.18	Slab	Sub angular	Rough
60	2.5	14.8	22.0	305.4	74.8	819.2	792.3	0.31	13.3	28.7	2.8	32.6	0.09	Discoid (plat)	Sub angular	Relatively smooth

Table 5. Particle dimensions, area, perimeter, surface area, volume, circumscribed and inscribed circle and circumscribed and inscribed sphere, Wadell roundness, inscribed-circumscribed sphere ratio and roundness,

5. Conclusion

The shape of gravel with different grain shapes was measured and described in two and three dimensional concepts. Based on the provided results of image processing and micro-CT scan for two and three-dimensional inspections, the following results can be stated:

1. The chosen spherical particles were classified under six groups and six particles were placed in each category. However, ellipsoid particles were classified as four groups where six grains were placed in each. Three dimensional images, particle projection and evaluation parameters were presented for entire grains, which can be used further for visual comparison in practice.

2. Particle shapes were assessed by performing two and three-dimensional approaches. Nevertheless, the results of 2D methods did not match the actual particle characteristics.

3. For the 3D calculation of sphericity, inscribed-circumscribed sphere ratio, the relationship $\psi_{i-c} = \dfrac{d_i}{d_c}$ was presented. This method demonstrated a very good agreement with the actual shape of spherical and flat particle as well as ellipsoid and elongated particles.

4. The proposed sphericity ratio was compared with other sphericity and form correlations. φ_0 indicated similar sphericity for particle with an identical outline, and do not produce similar results with ψ_{i-c}. The results revealed that Aschenbrenner, Krumbein, *Sneed* and Folk, Corey shape factors, Wentworth flatness index, elongation and flatness ratio and ψ_{i-c} offered the highest values of sphericity, respectively.

5. A new sphericity class was proposed for general particle form. A tabulated approach was provided using the mentioned classifications and Wadell's method for particle roundness. Further, a qualitative classification was suggested for particle surface roughness, by which qualitative and quantitative description of the particle shapes could be presented.

6. It was observed that while the sphericity, roundness and roughness varied, 2D parameters could not demonstrate these variations correctly. Also, the particle projection changed according to the particle rotation or image capture direction. 2D parameters were unable to show the changes in particle sphericity, roundness and roughness. For particle shape assessment, it is recommended to use suggested charts instead of 2D parameters. The proposed diagrams can be used for a rough estimation and the image processing technique as a more precise method which

can be used to describe and quantify the particle shape.

References

[1]   Altuhafi FN, Coop MR, Georgiannou VN. Effect of Particle Shape on the Mechanical Behavior of Natural Sands. J Geotech Geoenvironmental Eng 2016; 142. doi:10.1061/(ASCE)GT.1943-5606.0001569.

[2]   Santamarina J, Cho G. Soil behaviour: The role of particle shape. Adv. Geotech. Eng. Proc. Skempt. Conf., 2004, p. 604–17.

[3]   Lee SJ, Lee CH, Shin M, Bhattacharya S, Su YF. Influence of coarse aggregate angularity on the mechanical performance of cement-based materials. Constr Build Mater 2019; 204:184–92. doi:10.1016/j.conbuildmat.2019.01.135.

[4]   Kuang D, Wang X, Jiao Y, Zhang B, Liu Y, Chen H. Influence of angularity and roughness of coarse aggregates on asphalt mixture performance. Constr Build Mater 2019; 200:681–6. doi:10.1016/j.conbuildmat.2018.12.176.

[5]   Mvelase GM, Gräbe PJ, Anochie-Boateng JK. The use of laser technology to investigate the effect of railway ballast roundness on shear strength. Transp Geotech 2017; 11:97–106. doi:10.1016/j.trgeo.2017.05.003.

[6]   Guo Y, Markine V, Zhang X, Qiang W, Jing G. Image analysis for morphology, rheology and degradation study of railway ballast: A review. Transp Geotech 2019; 18:173–211. doi:10.1016/j.trgeo.2018.12.001.

[7]   Barrett PJ. The shape of rock particles, a critical review. Sedimentology 1980; 27:291–303. doi:10.1111/j.1365-3091.1980.tb01179.x.

[8]   Mitchell J, Soga K. Fundamentals of soil behavior. Third edit. John Wiley & Sons; 2005.

[9]   Sneed ED, Folk RL. Pebbles in the Lower Colorado River, Texas a Study in Particle Morphogenesis. J Geol 1958;66:114–50. doi:10.1086/626490.

[10]   Wentworth CK. The shapes of beach pebbles. vol. 131–C. 1922. doi:10.3133/pp131C.

[11]   Krumbein WC. Measurement and Geological Significance of Shape and Roundness of Sedimentary Particles. J Sediment Res 1941;11:64–72. doi:10.1306/D42690F3-2B26-11D7-8648000102C1865D.

[12]   Rodriguez J, Edeskär T, Knutsson S. Particle Shape Quantities and Measurement Techniques - A review. Electron J Geotech Eng 2013;18:169–98.

[13]   Nie Z, Liang Z, Wang X. A three-dimensional particle roundness evaluation method. Granul Matter 2018;20:1–11. doi:10.1007/s10035-018-0802-5.

[14]   Wang L, Wang X, Mohammad L, Abadie C. Unified Method to Quantify Aggregate Shape Angularity and Texture Using Fourier Analysis. J Mater Civ Eng 2005;17:498–504. doi:10.1061/(ASCE)0899-1561(2005)17:5(498).

[15]   Su D, Yan WM. Prediction of 3D size and shape descriptors of irregular granular particles from projected 2D images. Acta Geotech 2019;3. doi:10.1007/s11440-019-00845-3.

[16]   Wadell H. Sphericity and Roundness of Rock Particles. J Geol 1933;41:310–31. doi:10.1086/624040.

[17]   Lees G. A new Method for Determining the Angularity of Particles. Sedimentology 1964;3:2–21. doi:10.1111/j.1365-3091.1964.tb00271.x.

[18]   Zheng J, Hryciw RD. Traditional soil particle sphericity, roundness and surface roughness by computational geometry. Géotechnique 2015;65:494–506. doi:10.1680/geot.14.P.192.

[19]   Zingg T. Beitrag zur Schotteranalyse. Schweiz Miner Petrogr Mitt 1935;15:39–140.

[20]   ASTM D 2488-00. Standard practice for description and identification of soils (visual manual procedure). ASTM Int West Conshohocken, PA, 2000. doi:10.1520/D2488-00.

[21]   Blott SJ, Pye K. Particle shape: a review and new methods of characterization and classification. Sedimentology 2007;55:31–63. doi:10.1111/j.1365-3091.2007.00892.x.

[22]   Garboczi EJ, Liu X, Taylor MA. The 3-D shape of blasted and crushed rocks: From 20 μ m to 38 mm. Powder Technol 2012;229:84–9. doi:10.1016/j.powtec.2012.06.012.

[23]   Wadell H. Volume, Shape, and Roundness of Rock Particles. J Geol 1932;40:443–51. doi:10.1086/623964.

[24]   Wadell H. Volume, Shape, and Roundness of Quartz Particles. J Geol 1935; 43:250–80.

doi:10.1086/624298.

[25] Corey AT. Influence of shape on fall velocity of sand grains. MSc thesis, Colorado A&M College, 1949.

[26] Aschenbrenner BC. A new method of expressing particle sphericity. SEPM J Sediment Res 1956; 26:15–31. doi:10.1306/74D704A7-2B21-11D7-8648000102C1865D.

[27] Clayton C, Abbireddy C, Schiebel R. A method of estimating the form of coarse particulates. Geotechnique 2009;59:493–501. doi:10.1680/geot.2007.00195.

[28] Cox EP. A method of assigning numerical and percentage values to the degree of roundness of sand grains. J Paleontol 1927;1:179–83.

[29] Tickell FG. The Examination of Fragmental Rocks. Stanford University Press, Stanford, California: 1931.

[30] Riley NA. Projection Sphericity. J Sediment Res 1941;11:94–7. doi:10.1306/D426910C-2B26-11D7-8648000102C1865D.

[31] Janoo VC. Quantification of shape, angularity, and surface texture of base course materials. US Army Corps Eng 1998:22.

[32] Hryciw RD, Zheng J, Shetler K. Particle Roundness and Sphericity from Images of Assemblies by Chart Estimates and Computer Methods. J Geotech Geoenvironmental Eng 2016;142. doi:10.1061/(ASCE)GT.1943-5606.0001485.

[33] Zhou B, Wang J, Wang H. Three-dimensional sphericity, roundness and fractal dimension of sand particles. Géotechnique 2018;68:18–30. doi:10.1680/jgeot.16.P.207.

[34] Kuo C, Freeman RB. Image Analysis Evaluation of Aggregates for asphalt concrete Mixture. Transp Res Rec 1998;1615:65–71. doi:https://doi.org/10.3141/1615-09.

[35] Masad E, Olcott D, White T, Tashman L. Correlation of fine aggregate imaging shape indices with asphalt mixture performance. Transp Res Rec 2001;1757:148–56. doi:10.3141/1757-17.

[36] Masad E, Button JW. Unified Imaging Approach for Measuring Aggregate Angularity and Texture. Comput Civ Infrastruct Eng 2000;15:273–80. doi:10.1111/0885-9507.00191.

[37] Koohmishi M, Palassi M. Evaluation of morphological properties of railway ballast particles by image processing method. Transp Geotech 2017;12:15–25. doi:10.1016/j.trgeo.2017.07.001.

[38] Pan T, Tutumluer E. Evaluation of Visual Based Aggregate Shape Classifications Using the University of Illinois Aggregate Image Analyzer (UIAIA). Pavement Mech Perform 2006;GSP 154:203–11. doi:10.1061/40866(198)26.

[39] Vallejo LE. Fractal analysis of granular materials. Géotechnique 1995;45:159–63. doi:10.1680/geot.1995.45.1.159.

[40] Su D, Yan WM. Quantification of angularity of general-shape particles by using Fourier series and a gradient-based approach. Constr Build Mater 2018;161:547–54. doi:10.1016/j.conbuildmat.2017.12.004.

[41] Hyslip JP, Vallejo LE. Fractal analysis of the roughness and size distribution of granular materials. Eng Geol 1997;48:231–44. doi:10.1016/S0013-7952(97)00046-X.

[42] Araujo GS, Bicalho K V, Tristão FA. Use of digital image analysis combined with fractal theory to determine particle morphology and surface texture of quartz sands. J Rock Mech Geotech Eng 2017;9:1131–9. doi:10.1016/j.jrmge.2017.06.004.

[43] Ravanshad A, Roque R, Tebaldi G, Lopp G, Carpinone PL. Evaluation of Two-Dimensional Gray-Scale Images for Microtexture Analysis of Aggregate Surface. J Mater Civ Eng 2016;28:04016044. doi:10.1061/(ASCE)MT.1943-5533.0001520.

[44] Su D, Wang X, Yang H-W, Hong C. Roughness analysis of general-shape particles, from 2D closed outlines to 3D closed surfaces. Powder Technol 2019;356:423–38. doi:10.1016/j.powtec.2019.08.042.

[45] Yang X, Chen S, You Z. 3D Voxel-Based Approach to Quantify Aggregate Angularity and Surface Texture. J Mater Civ Eng 2017;29:04017031. doi:10.1061/(ASCE)MT.1943-5533.0001872.

[46] Kuo CY, Rollings RS, Lynch LN. Morphological Study of Coarse Aggregates Using Image Analysis. J Mater Civ Eng 1998;10:135–42. doi:10.1061/(ASCE)0899-1561(1998)10:3(135).

[47] Bowman ET, Soga K, Drummond W. Particle shape characterisation using Fourier descriptor analysis. Géotechnique 2001;51:545–54. doi:10.1680/geot.51.6.545.40465.

[48] Goudie A. Geomorphological techniques. second edi. routledge; 1990.

[49] Powers M. C. A New Roundness Scale for Sedimentary Particles. SEPM J Sediment Res 1953;Vol. 23:117–9. doi:10.1306/D4269567-2B26-11D7-8648000102C1865D.

[50] Krumbein WC, Sloss LL. Stratigraphy and Sedimentation. Second Edi. San Francisco: W.H. Freeman and

Company; 1963.

[51] Cho G chun, Dodds J, Santamarina JC. Particle Shape Effects on Packing Density , Stiffness and Strength: Natural and Crushed Sands. J Geotech Geoenvironmental Eng 2006;132:591–602. doi:10.1061/(ASCE)1090-0241(2006)132:5(591).

[52] Xiong Q, Jivkov AP. Analysis of pore structure effects on diffusive transport in Opalinus clay via pore network models. Mineral Mag 2015;79:1369–77. doi:10.1180/minmag.2015.079.6.12.

[53] Xiong Q, Baychev TG, Andrey J. Review of pore network modelling of porous media: Experimental characterisations, network constructions and applications to reactive transport. J Contam Hydrol 2016;192:101–17. doi:10.1016/j.jconhyd.2016.07.002.

[54] Su D, Yan WM. 3D characterization of general-shape sand particles using microfocus X-ray computed tomography and spherical harmonic functions, and particle regeneration using multivariate random vector. Powder Technol 2018;323:8–23. doi:10.1016/j.powtec.2017.09.030.

[55] Zhao B, Wang J. 3D quantitative shape analysis on form, roundness, and compactness with µCT. Powder Technol 2016;291:262–75. doi:10.1016/j.powtec.2015.12.029.

[56] Zheng J, Hryciw RD. Soil particle size and shape distributions by stereophotography and image analysis. Geotech Test J 2017;40:317–28. doi:10.1520/GTJ20160165.

[57] Rueden CT, Schindelin J, Hiner MC, DeZonia BE, Walter AE, Arena ET, et al. ImageJ2: ImageJ for the next generation of scientific image data. BMC Bioinformatics 2017;18:529. doi:10.1186/s12859-017-1934-z.

[58] Cybermed Inc. Operating manual, OnDemand3D application 2015:178.

[59] Zhao B, Wang J. 3D quantitative shape analysis on form, roundness, and compactness with µCT. Powder Technol 2016;291:262–75. doi:10.1016/j.powtec.2015.12.029.

[60] 3Dim Laboratory s.r.o. 3DimViewer 3.1.1 2017.

[61] Nie Z, Liang Z, Wang X, Gong J. Evaluation of granular particle roundness using digital image processing and computational geometry. Constr Build Mater 2018;172:319–29. doi:10.1016/j.conbuildmat.2018.03.246.

[62] Porter JJ. Electron Microscopy of Sand Surface Texture. SEPM J Sediment Res 1962;Vol. 32:124–35. doi:10.1306/74D70C59-2B21-11D7-8648000102C1865D.

[63] Barksdale RD, Itani SY. Influence of aggregate shape on base behavior. Transp Res Rec 1989;1227:173–82.

[64] ASTM D 5821-13. Standard Test Method for determining the percentage of fractured particles in coarse aggregate. ASTM Int West Conshohocken, PA, 2017. doi:10.1520/D5821-13R17.

[65] BS 812 Part 1. Methods of Determination of Particle Size and Shape. Br Stand Inst 1975.